

DOI: <https://doi.org/10.37434/tpwj2023.08.06>

# MODERN TECHNOLOGIES OF ELECTROPHYSICAL TREATMENT FOR REGULATION OF STRESS-STRAIN STATES OF ELEMENTS OF WELDED STRUCTURES

**L. Lobanov, M. Pashchyn, O. Mikhodui**

E.O. Paton Electric Welding Institute of the NASU  
11 Kazymyr Malevych Str., 03150, Kyiv, Ukraine

## ABSTRACT

The development of industry stimulates the development of modern approaches to the optimization of welded structures. The use of pulsed electromagnetic fields, plasma currents, electrodynamic forces and their combined effects is a new trend in engineering practice. Treatment with a pulsed electromagnetic field (TPEMF) is a promising direction for optimizing the stress-strain states (SSS) of welded joints (WJ) made of non-ferromagnetic metal materials. Using the method of electron speckle interferometry, the effect of TPEMF on the SSS of samples of circumferential WJ with a thickness of  $\delta = 1.0$  mm from aluminium alloy AMg6 was investigated. The kinetics of the action of the force  $P$  of the magnetic field pressure on the residual displacements  $f$  and SSS of the samples during their TPEMF were investigated. TPEMF of WJ samples was performed without and with the use of an additional screen ( $\delta = 5.0$  mm) contributes to the reduction of  $f$  values by 2 and 4 times, respectively, and residual SSS by 50 and 80 %. The advantages of using electrodynamic treatment (EDT) of butt 3.0 mm alloy AMg61 (1561) in the TIG welding process are substantiated. It was proved that EDT during TIG contributes to the formation of peak values of residual compressive stresses in the weld zone by 60 % more than EDT during room temperature ( $T_k$ ). The use of a pulsed barrier discharge (PBD), which generates a low-temperature plasma on the surface of the metal, contributes to the optimization of its structure. An increase in the hardness of  $HV$  structural steel 25KhGNMT as a result of its PBD treatment from 420 to 510 units was established.

**KEYWORDS:** treatment of welded joints, pulsed magnetic field, pulsed barrier discharge; electrodynamic treatment, aluminium alloy, structural steel, residual displacements, stress-strain state, hardness of steel

## INTRODUCTION

The development of modern industry requires the study of progressive energy-saving technologies to improve the service properties of metal structures. In this regard, the development of methods of treatment of metal materials and welded joints based on the effect of a pulsed electromagnetic field is challenging. These include electrodynamic treatment (EDT), treatment with a direct action (pressure) of a pulsed electromagnetic field (TPEMF) and a pulsed barrier discharge (PBD) [1–6]. Based on EDT and TPEMF, technologies for control of the stress-strain state of thin-sheet welded joints are developed. Taking into account the results [1], a promising technology of EDT in the process of welding has been developed, which provides the following advantages over EDT after welding:

- effect of the thermal cycle of welding contributes to more intensive relaxation of welding stresses as a result of EDT compared to treatment of weld metal at room temperature;

- reduction in the labour intensity of manufacturing welded structure due to the transition from successive to simultaneous performance of technological operations of welding and EDT. The use of PBD

opens up new opportunities to improve the hardness of structural steels for special equipment.

## AIM OF THE WORK

Is the study of TPEMF, EDT and PBD effect on residual stresses and mechanical characteristics of metal materials and welded joints.

## RESEARCH PROCEDURE AND MATERIALS

Electrophysical models, which form the basis of the action of TPEMF, EDT and PBD on metals, alloys and welded joints, are presented respectively in [4], [1] and [6]. Electrophysical characteristics of electrode systems and power sources for TPEMF, EDT and PBD are presented, respectively, in [2, 4, 5], [1, 3] and [6].

As a tool for TPEMF realization, a plane inductor (Figure 1, a) was used, and to evaluate the efficiency of treatment, plane specimens of AMg6 aluminium alloy in the form of a disc were used, whose thickness and diameter were respectively  $\delta = 1.0$  mm and  $D_{sp} = 90$  mm (Figure 1, b). During treatment, a current-conducting shield in the form of a disc from AMg6 alloy was used, its diameter and thickness were respectively 90 and 5.0 mm (Figure 1, c). Circumferential welds were produced by TIG method in Ar environment along the line of the circle with a diameter

Copyright © The Author(s)

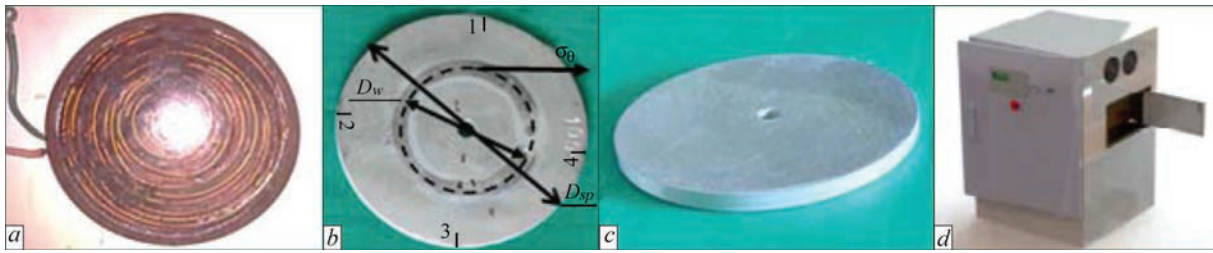


**Figure 1.** Appearance: *a* — plane inductor; *b* — specimen of circumferential welded joint of AMg6 alloy with a thickness  $\delta = 1.0$  mm, where  $D_{sp} = 90$  mm and  $D_w = 45$  mm are respectively the diameters of the specimen and the weld,  $\sigma_\theta$  is the component of residual stresses; *c* — current-conducting shield with a diameter of 90 mm and a thickness of 5 mm; *d* — PS for TPEMF

$D_w = 45$  mm. A tangent component  $\sigma_\phi$  (Figure 1, *b*) of residual stressed state of welded joints and vertical movements  $f$  of the discs' edges before and after TPEMF were evaluated by the method of electron and speckle-interferometry.

To realize the discharge cycles of TPEMF, the power source (PS) was used based on a capacitor system with a charging voltage  $U$  of up to 800 V and pulsed current amplitude of up to 10 kA (Figure 1, *d*). PS can perform TPEMF in an automatic mode with 1–5 s time periods between the pulses. The registration of time distributions of the pulsed current  $I$  and the power of electrodynamic pressure  $P$  at TPEMF of the specimens without and with the use of a shield was performed using a non-inductive shunt and an accelerometer Kistler Instrumente AG, respectively [7]. TPEMF was performed on the specimens with the thickness  $\delta = 1.0$  mm and on the assembly of the specimen  $\delta = 1.0$  mm with a current-conducting shield  $\delta = 5.0$  mm ( $\Sigma\delta = 6$  mm). Treatment was carried out by the series of EPC on the mode at a charging voltage  $U$  of up to 800 V. Residual stressed states of welded joints were studied using the electron and speckle-interferometry method [1].

The hardware complex for automatic welding of aluminium alloys in the EDT process has been developed and manufactured (Figure 2). The complex includes system for feeding filler wire 1, torch 2 for

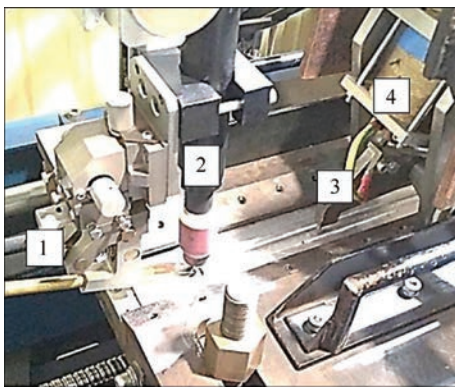


**Figure 2.** Hardware complex for automatic TIG welding, which is compatible with EDT of a weld, where 1 — system for feeding filler wire; 2 — welding torch; 3 — electrode device; 4 — linear solenoid for movement of EDT electrode

TIG welding, electrode device for EDT 3 and linear solenoid for movement 4 of electrode for EDT. The components of the complex are structurally combined into a monoblock.

Mathematical modeling of stress-strain states of welded joints as a result of EDT was performed in the conditions of elevated temperatures (in the process of welding), with the use of a simplified two-dimensional (2D) planar formulation. The design diagram of the problem of the process of impact interaction of the electrode-indenter with plates [8] is presented in Figure 3. The solution of the problem was performed using ANSYS/LS-DYNA software.

PBD treatment of the surface of specimens of 25KhGNMT steel was performed using an electrode system (ES), the structural diagram of which is shown in Figure 4.

The diagram of the electrode system (ES) for PBD treatment is shown in Figure 4, *a*. ES consisted of studied specimen 1 of 25KhGNMT steel, high-voltage electrode 2 and glass (quartz glass) dielectric barrier 3 ( $100 \times 100 \times 1$  mm<sup>3</sup>). To reduce the edge effect, electrode 2 had rounded edges. The treatment was carried out at a gas gap  $\delta$  of 1 mm thickness between plate 1 and barrier 3. High voltage (HV) was supplied to electrode 2 from the pulse generator (PG), which provided unipolar pulses of a voltage with an amplitude of up to 30 kV at their rising rate  $\approx 3 \cdot 10^{11}$  V/s and a duration of about 150 ns. The appearance of the dis-

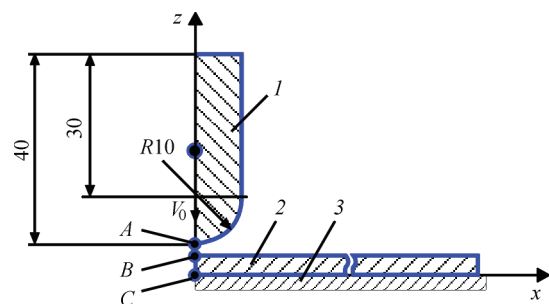


**Figure 3.** Design diagram of the process of dynamic loading of a plate at EDT: 1 — electrode-indenter; 2 — specimen being treated; 3 — absolutely rigid base, *A* — point on the outer surface of the electrode-indenter; *B* — point on the outer surface of a plate; *C* — point on the back surface of a plate;  $V_0$  — speed of movement of the electrode-indenter

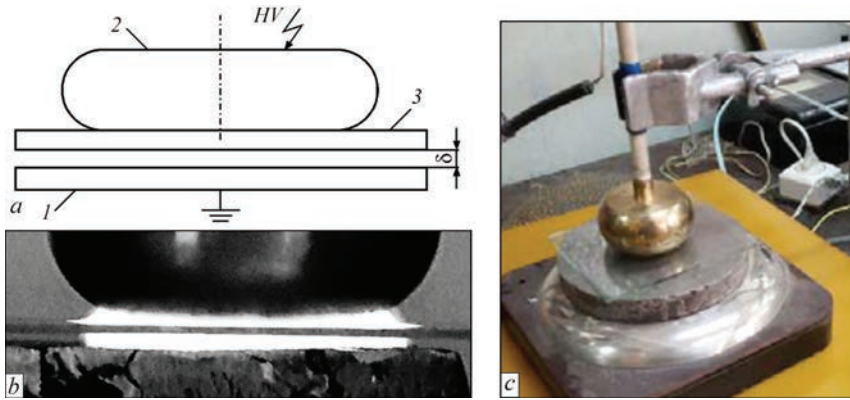


**Figure 4.** PBD treatment of 25KhGNMT steel, where: *a* — diagram of electrode system for PBD treatment of specimens of 25KhGNMT steel, where *l* — studied specimen 1 of 25KhGNMT steel; 2 — high-voltage electrode; 3 — dielectric barrier;  $\delta$  — gas gap; *HV* — high voltage; *b* — appearance of PBD; *c* — appearance of PBD treatment process of 25KhGNMT steel

charge, shown in Figure 4, *b* (exposure time is 0.1 s) indicates a homogeneous nature in the gap  $\delta$  rather than thredlike.

**DISCUSSION OF RESEARCH RESULTS**

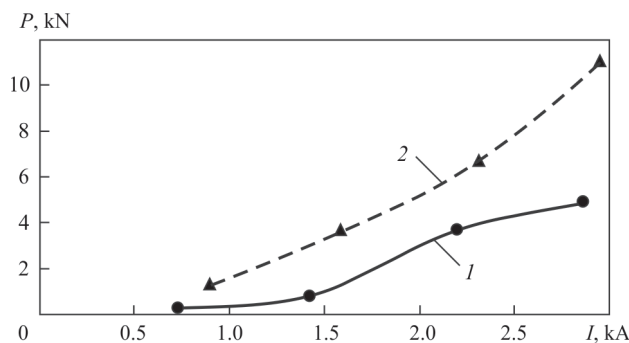
Dependence of pressure force *P* at TPEMF on current *I* for different thickness  $\delta$  of the specimens is shown in Figure 5. Based on its data, in the studied range of treatment modes, it is possible to see that with an increase in  $\delta$ , *P* will grow, because it is defined as an integral value in a certain volume of a current-conductive medium. At an increase in  $\delta$  to 6.0 mm as a result of using a shield (curve 2), the values *P* rise twice compared to TPEMF of the specimens  $\delta = 1.0$  mm without a shield (curve 1).

The efficiency of TPEMF effect on the residual forming of the specimens treated under the above-mentioned conditions confirm the data given in Figure 4, *a-c*. The values of vertical movements of the discs' edges *f* (Figure 6, *a*) were recorded at the points Nos 1–4 (Figure 6, *c*) with a fixed angular distance  $l_\alpha$  of 90° between the adjacent points. Performance of TPEMF without a shield (Figure 6, *d*, curve 2) and with its use (curve 3) allows reducing the values of movements *f* of the discs' edges relatively by up to

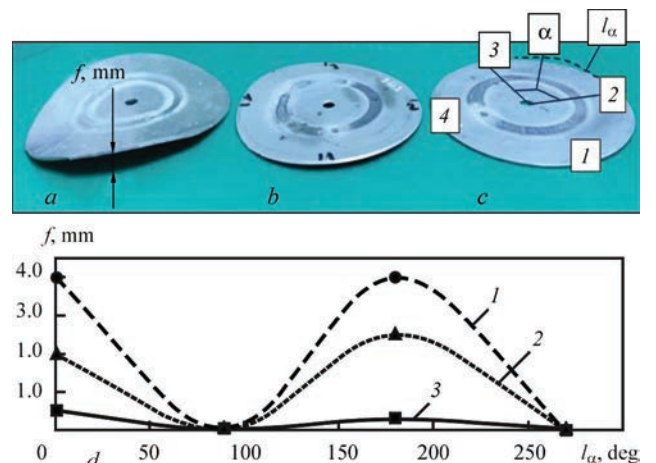
two or eight times compared to the specimens that were not subjected to TPEMF.

Figure 7 shows the results of TPEMF effect on the component  $\sigma_\theta$  of residual stresses in the centre of the weld (W) and in the area near weld zone (NWZ) at a distance of 10 mm from the weld line. Taking into account the bending of the discs (Figure 6), which results in the imbalance of the diagrams of residual stresses, as an evaluation of TPEMF effect on the stressed state, the peak values  $\sigma_\theta$  were determined in W and in NWZ in the specimens in the initial state and under the set treatment conditions. It is possible to see that in general TPEMF has a positive effect on the residual stressed state of the circumferential welded joints of AMg6 alloy with a thickness  $\delta = 1$  mm.

Though initial (before TPEMF) values  $\sigma_\theta$  during treatment without a shield (*a*) and with a shield (*c*) differ, which is associated with a low rigidity of the



**Figure 5.** Influence of amplitude EPC values — *I* on pressure force *P* at TPEMF of specimens of circumferential welded joints  $\delta = 1.0$  mm of AMg6 alloy; curve 1 — TPEMF without a shield; curve 2 — TPEMF with a shield



**Figure 6.** Residual forming of circumferential welded joints of AMg6 alloy, where: *a* — appearance (*A*) of the disc without treatment, where *f* is the movement of the disc's edges; *b* — *A* after TPEMF without a shield; *c* — *A* after TPEMF with a shield, where 1–4 is the number of point of movement measurement,  $\alpha$  and  $l_\alpha$  are respectively the angle and angular distance between the points 2–3; *d* — vertical movements *f* of the disc's edges, where curve 1 — without TPEMF; 2 — after TPEMF without a shield; 3 — after TPEMF with the use of a shield

discs, it can be seen that the use of a shield has a positive effect on relaxation of stresses in TPMEF. This is confirmed by comparing the diagrams between each other (*a-b*) and (*c-d*). Thus, the treatment without and with the use of a shield led to a decrease in the initial values  $\sigma_0$  in the active zone of tension (W) respectively by 36 and 56 %, and in the zone of reactive compression (NWZ) — by 50 and 80 %.

The results of mathematical modeling are shown in Figure 8, from which it can be seen that EDT in the conditions of heating the plate from AMg61 alloy to the temperature  $T = 150\text{ }^\circ\text{C}$  (thermoelasticity), provides larger values of longitudinal (along the axis  $X$  in Figure 3) compression  $\sigma_x$  stresses, than at  $T = 20\text{ }^\circ\text{C}$  (room) and at  $T = 300\text{ }^\circ\text{C}$  (thermoelasticity). This allows choosing the distance between welding torch 2 and electrode 3 for EDT (Figure 2) that provides the optimum level of residual compression  $\sigma_x$  in the weld joint.

Verification of modeling results was carried out on the specimens of butt joints from AMg61 alloy with the sizes of  $300 \times 200 \times 3\text{ mm}$  (Figure 9), where the Specimen No. 1 was not subjected to EDT, the Specimen No. 2 was subjected to EDT at  $T = 20\text{ }^\circ\text{C}$  and the Specimen No. 3 was subjected to EDT at  $T = 150\text{ }^\circ\text{C}$ . The values of residual longitudinal deflections  $f_x$  of the specimens and residual  $\sigma_x$  confirm both the efficiency of EDT, as well as its growth in the conditions of thermal deformation welding cycle. In the Specimen No. 2, the values  $f_x$  are reduced by 1.8 times compared to the Specimen No. 1, and in the Specimen No. 3 — by 3.7 (Figure 9, *a*). The values of the membrane tensile  $\sigma_x$  (curve 2 in Figure 9, *b-d*) in the weld centre on the Specimen No. 2 compared to the Specimen No. 1 are reduced by 95 % (Figure 9, *c*), and in the Specimen No. 3 they are transformed into compression and amount to about  $0.3\sigma_{0.2}$  for AMg61 alloy (Figure 9, *d*).

It was found that the maximum effect of PBD on the hardness of 25KhGNMT steel is achieved when duration of the specimens treatment is 15 minutes (at the optimal mode). In this case, the values of  $HV$  hardness after the treatment increase by 20 % from 420 to 505  $\text{kg/mm}^2$  (Figure 10, *a*). In depth from the treated surface (from 0 to 2200  $\mu\text{m}$ ) in the cross-section of the specimen, the changes in structural and phase composition, parameters of thin structure and dislocations density were revealed. In depth from the treated surface to 300  $\mu\text{m}$ , exclusively the structure of tempered martensite and lower bainite is formed during its refinement and a uniform distribution of dislocations density  $\rho = (2-8) \cdot 10^{10}\text{ cm}^{-2}$  (Figure 10, *b*). The obtained results indicate that PBD facilitates an improvement in the dynamic strength of welded

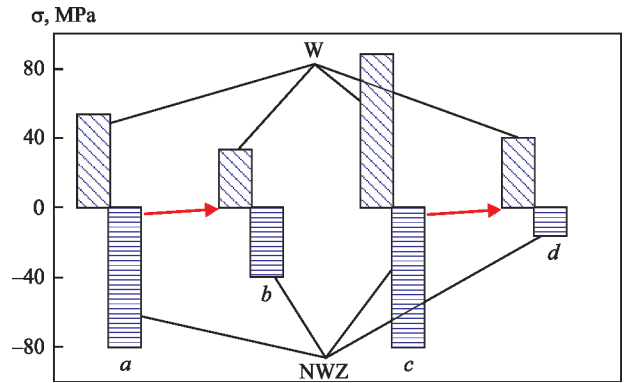


**Figure 7.** Influence of TPMEF on the component  $\sigma_0$  of residual stresses in the welds (W) and in the NWZ of circumferential welded joints of the specimens of AMg6 alloy with a thickness  $\delta = 1\text{ mm}$ : *a* — peak values  $\sigma_0$  of the specimens in the initial state; *b* —  $\sigma_0$  after TPMEF without the use of a shield; *c* —  $\sigma_0$  specimens in the initial state; *d* —  $\sigma_0$  after TPMEF with the use of a shield

structures of the mentioned steel during their contact interactions.

Analyzing the abovementioned results, it should be noted that TPMEF, EDT in the process of welding and local PBD treatment of metals, alloys and welded joints is the basis for the development of a number of

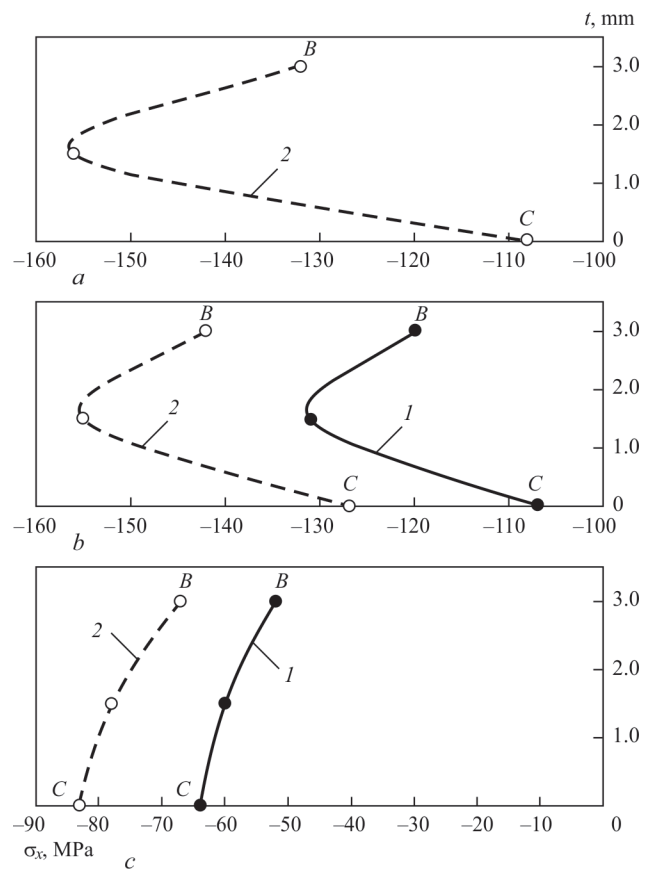


**Figure 8.** Results of modeling stresses  $\sigma_x$  along the line between the points B and C (Figure 3) of the plates of AMg61 alloy  $\delta = 3\text{ mm}$  after EDT at the temperature  $T$  and cooling to  $T = 20\text{ }^\circ\text{C}$ , where curve 1 —  $\sigma_x$  (instant) at the moment of completion of contact interaction at elevated temperatures; curve 2 —  $\sigma_x$  at room temperature: *a* —  $T = 20\text{ }^\circ\text{C}$ ; *b* —  $T = 150\text{ }^\circ\text{C}$ ; *c* —  $T = 300\text{ }^\circ\text{C}$

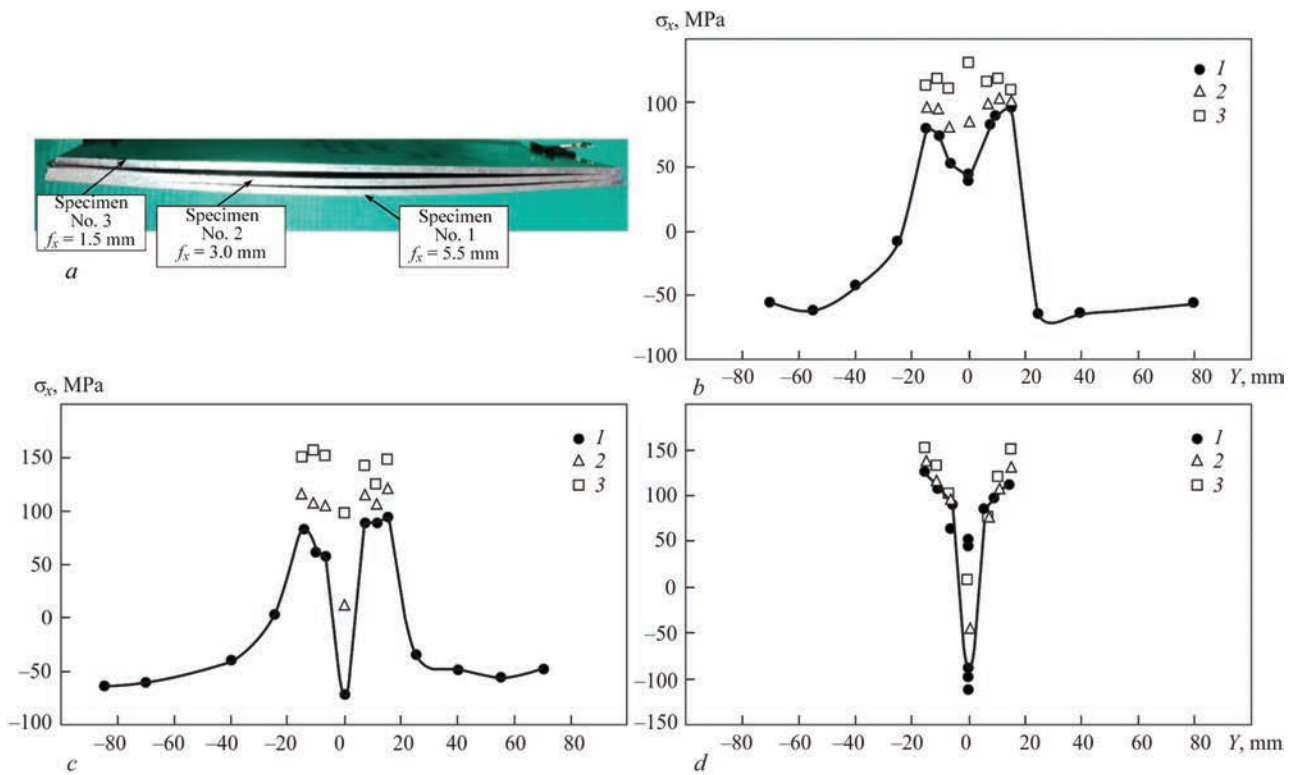


**Figure 9.** Longitudinal deflections  $f_x$  and residual stresses  $\sigma_x$  of the specimens of welded joints of AMg61 alloy of  $\delta = 3$  mm, where the Specimen No. 1 — no EDT, Specimen No. 2 — EDT at  $T = 20$  °C, Specimen No. 3 — EDT at  $T = 150$  °C: *a* — appearance and values of  $f_x$  of the Specimens Nos 1–3; *b* — distribution of  $\sigma_x$  at the central cross-section of the Specimen No. 1, where curve 1 — top (●) surface of the point B in Figure 3, curve 2 — membrane stresses; 3 — bottom (□) surface of the point B in Figure 3; *c* — similarly to (b) for the Specimen No. 2; *d* — similarly to (b) for the Specimen No. 3

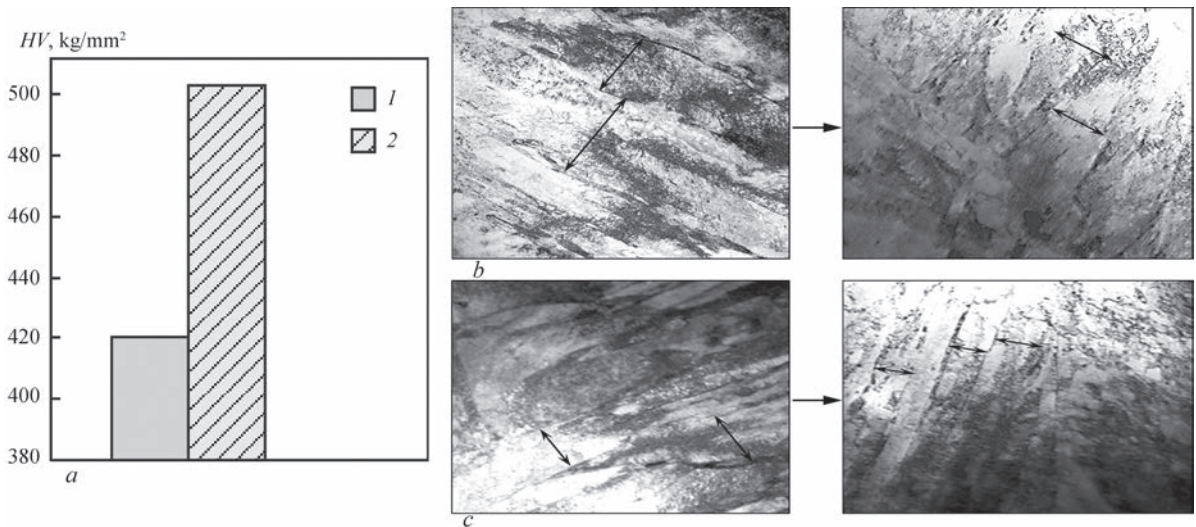


**Figure 10.** Influence of PBD treatment on the structure of 25KhGNMT steel: *a* — values of Vickers hardness ( $HV$ ) before and after PBD treatment; thin structure before and after PBD treatment; *b* — tempered martensite ( $M_{temp}$ ) before and after PBD treatment; *c* — lower bainite ( $B_l$ ) before and after PBD

technologies aimed at optimizing welded structures of new equipment.

### CONCLUSIONS

1. It was found that treatment with a pulsed electromagnetic field (TPEMF) allows reducing residual displacements and stresses of the specimens of circumferential welded joints from AMg6 alloy by up to eight times compared to untreated ones.

2. On the basis of mathematical modeling and experimental studies, it was proved that the use of electrodynamic treatment (EDT) of weld metal, which is performed in a single process synchronously with arc welding is more effective compared to separate EDT after welding, which is expressed in a more optimal residual stress-strain state of a finished welded joint of the aluminium AMg61 alloy.

3. It was found that as a result of treatment of 25KhGNMT steel with a pulsed barrier discharge (PBD), its Vickers hardness ( $HV$ ) is increased by 20 % — from 420 to 505 kg/mm<sup>2</sup>, which spreads to a depth of up to 2 mm and is accompanied by dispersion of the treated structure.

**REFERENCE**

1. Lobanov, L., Kondratenko, I., Zhiltsov, A. et al. (2018) Development of post-weld electrodynamic treatment using electric current pulses for control of stress-strain states and improvement of life of welded structures. *Mater. Performance and Charact.*, 7(4), 941–955. DOI: <https://doi.org/10.1520/MPC20170092>
2. Dubodelov, V.I., Goruk, M.S. (2018) The use of electromagnetic fields and magnetodynamic phenomena to intensify the effect on metal systems. World and Ukrainian experience. *Materials Science: Achievements and Prospects*, Vol. 2, Kyiv, Akadempriodyka, 24–50 [in Ukrainian].
3. Zhang, Jun, Liu, Ji-De, Zhang, Xin-Fang et al (2021) Effect of high density current pulses on microstructure and mechanical properties of dual-phase wrought superalloy. *Acta Metallurgica Sinica*, 34(12), 1635–1644. DOI: <https://doi.org/10.1007/s40195-021-01211-7>
4. Qin, Shuyang, Zhang, Xinfang (2022) Ultrafast regulation of nano-scale matrix defects using electrical property discrepancies to delay material embrittlement. *J. of Mater. Sci. and Technol.*, 119, 25–3620. DOI: <https://doi.org/10.1016/j.jmst.2021.11.070>
5. Guo, J.D., Wang, X.L., Dai, W.B. (2015) Microstructure evolution in metals induced by high density electric current

pulses. *Mater. Sci. and Technol.*, 31 (13a), 1545–1554. DOI: <https://doi.org/10.1179/1743284715Y.0000000001>

6. Zhang, Xinfang, Qin, Rongshan (2018) Exploring the particle reconfiguration in the metallic materials under the pulsed electric current. *Steel Research Intern. Open Access*, 89(12) Article number 1800062. DOI: <https://doi.org/10.1002/srin.201800062>
7. *Quartz Accelerometer 8042*. Kistler Instrumente AG. <https://www.datasheetarchive.com/kistler-datasheet.html>

**ORCID**

L.M. Lobanov: 0000-0001-9296-2335,  
 M.O. Pashchyn: 0000-0002-2201-5137,  
 O.L. Mikhodui: 0000-0001-6660-7540

**CONFLICT OF INTEREST**

The Authors declare no conflict of interest

**CORRESPONDING AUTHOR**

M. Pashchyn  
 E.O. Paton Electric Welding Institute of the NASU  
 11 Kazymyr Malevych Str., 03150, Kyiv, Ukraine.  
 E-mail: [svarka2000@ukr.net](mailto:svarka2000@ukr.net)

**SUGGESTED CITATION**

L. Lobanov, M. Pashchyn, O. Mikhodui (2023) Modern technologies of electrophysical treatment for regulation of stress-strain states of elements of welded structures. *The Paton Welding J.*, 8, 50–55.

**JOURNAL HOME PAGE**

<https://patonpublishinghouse.com/eng/journals/tpwj>

Received: 16.05.2023  
 Accepted: 07.08.2023

**SUPERHARD FUSED SPHERICAL TUNGSTEN CARBIDES**

**DEVELOPED IN PWI**



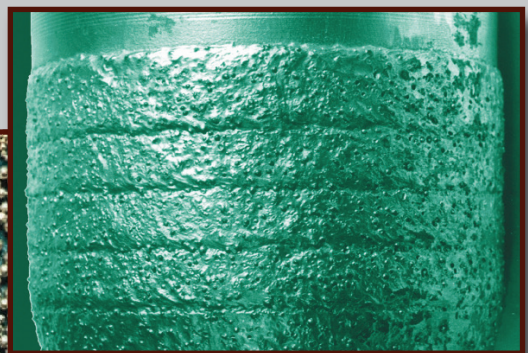
Drill pipe tool joint coated with spherical tungsten carbide



“Sfera-2500” machine for thermal centrifugal spraying



Appearance of spherical tungsten carbides



- Particle size, mm — 0.15–1.10
- Hardness,  $HV_{-0.1}$  — > 3000

Characteristic wear of drill bit teeth clad with tungsten carbide